GEOPHYSICAL RESEARCH LETTERS, VOL. 27, NO. 17, PAGES 2713-2716, SEPTEMBER 1, 2000

The Effect of Upper Ocean Eddies on the Non-Steric Contribution to the Barotropic Mode

Jay F. Shriver and Harley E. Hurlburt
Naval Research Laboratory, Stennis Space Center, Mississippi

Abstract. The non-steric contribution to sea surface height (SSH) variability hampers the use of satellite altimeter data in mapping steric-related variability. Here, two eddy-resolving 1/16° world ocean simulations are used to investigate the effects of mesoscale flow instabilities on the non-steric (or abyssal ocean) contribution to the global barotropic mode. Model results show the non-steric component accounting for > 50% of the total SSH variability over 37% of the world ocean in the model, predominantly at mid and high latitudes. Most of this is either wind-driven and deterministic or eddy-driven and nondeterministic. Upper ocean flow instabilities drive deep flows and generate non-steric SSH variability maxima (5 – 10 cm rms or more) in many major current systems throughout the world ocean. Resulting ocean anomalies are a nondeterministic response to atmospheric forcing and an eddy-resolving data-assimilative ocean model that demonstrates the essential dynamics is needed to depict their evolution.

Introduction

Recent work [*Hurlburt et al.*, 1996; *Hurlburt and Metzger*, 1998; *Hogan and Hurlburt*, 2000; *Hurlburt and Hogan*, 2000] has demonstrated the importance of high horizontal resolution and upper ocean - topographic coupling via flow instabilities for accurate simulation of current pathways in several parts of the world ocean. Very fine resolution of mesoscale variability is required to obtain sufficient coupling, 1/16° or more in most locations. Upper ocean - topographic coupling begins with unstable upper ocean currents where baroclinic instability plays an important role. Baroclinic instability is very efficient in transferring energy into the abyssal layer, resulting in upper ocean eddy-driven deep flows [*Holland and Lin*, 1975; *Rhines and Holland*, 1979] that follow the *f/h* contours of the bottom topography. These abyssal currents then strongly influence the pathways of upper ocean currents [*Hurlburt et al.*, 1996].

This energizing of the abyssal circulation by upper ocean eddy generation should impact the abyssal ocean (or non-steric) contribution to the barotropic mode and the corresponding contribution to sea surface height (SSH), but to what degree? Since SSH is measurable by satellite altimetry, this has implications for (1) analysis of altimetric SSH, (2) downward projection of the SSH data, (3) use of the data in ocean data synthesis and assimilation and (4) its use in defining initial states (including the abyssal ocean) for eddy-resolving ocean forecasting. In this paper the effect of eddies on the non-steric contribution to the global barotropic mode is investigated using a pair of world ocean simulations at 1/16° resolution. One is barotropic, the other includes baroclinicity and simulates vigorous and nearly ubiquitous mesoscale variability. Each of these simulations was forced 1979-97 with 6-12 hourly winds as described in the next section. The model used in this study is also discussed in the next section. The results and conclusions are discussed in subsequent sections.

Paper number 1999GL011105.

Model

The numerical ocean model used here is a primitive equation layered formulation where the equations have been vertically integrated through each layer. The model is a descendant of the one by *Hurlburt and Thompson* [1980], with greatly expanded capability [*Wallcraft*, 1991]. The model equations in spherical coordinates are discussed in *Moore and Wallcraft* [1998] and the scalable, portable computer code in *Wallcraft and Moore* [1997].

The two 1/16° model experiments are 1 layer barotropic (experiment BT1) and 6-layer with stratification in the vertical (experiment BT6). A modified version of the 1/12° ETOP05 bottom topography [*NOAA*, 1986] was used in the simulations. It was first interpolated to the model grid, then smoothed twice with a 9-point smoother to reduce energy generation at small scales that are poorly resolved by the model. The maximum depth was set at 6500 m and the minimum depth at 200 m (near the shelf break). The 200 m isobath was used as the model boundary with a few exceptions like the Tsugaru, Tsushima and Soya Straits which are required to connect the Sea of Japan with the Pacific Ocean. In the model integration the amplitude of the topography above a reference depth of 6500 m was multiplied by a fraction (0.69) to confine it to the lowest layer.

The model equations are integrated on a C-grid [*Mesinger and Arakawa*, 1976, see Chapter 4, p. 47] using a semi-implicit numerical scheme. Additional aspects of the model numerics are described in detail in *Hurlburt and Thompson* [1980], *Wallcraft* [1991] and *Moore and Wallcraft* [1998].

Each of the simulations was forced 1979-97 by 6-12 hourly 1000mb winds from the European Centre for Medium-Range Weather Forecasts [*ECMWF*, 1995; *Gibson et al.*, 1997] with the temporal mean replaced by the annual mean from the *Hellerman and Rosenstein* [1983] (HR) monthly wind stress climatology as discussed in *Metzger et al.* [1992]. The simulations were each initialized from climatological simulations that had been spun up to statistical equilibrium using HR as the wind forcing.

Results/Discussion

Suginohara [1981] discusses 2-layer ocean circulation model results in terms of an upper layer component and lower

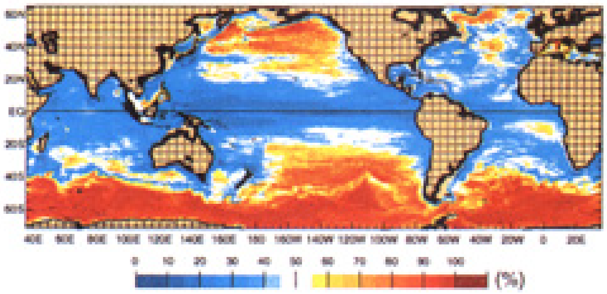

Figure 1. The fraction of total sea surface height (SSH) variability in simulation BT6 which is nonsteric. The units are in percent and the contour interval is 5 %.

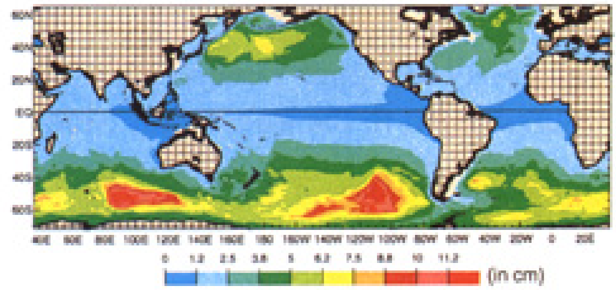

Figure 3. RMS SSH variability from simulation BT1. The units are cm and the contour interval is 1.25 cm.

layer component, where each of these components are fundamentally different dynamically. Within this section we partition the ocean similarly, describing the ocean circulation in terms of a steric and a non-steric component. The term steric is used to describe the thermal wind effects of stratification which occur in the upper 5 layers (surface to approximately 1500m depth) of the 6-layer model. The abyssal layer flow (~1500m to the sea floor) is non-steric and the abyssal layer pressure field can be used to calculate the non-steric contribution to sea surface height (SSH). As discussed in the introduction, previous work has shown that energizing of the non-steric circulation by upper ocean eddies can substantially affect current pathways via upper ocean-topographic coupling [e.g., *Hurlburt et al.*, 1996]. *Hurlburt and Metzger* [1998] even showed that an entire northern branch of the Kuroshio Extension could be explained by this mechanism.

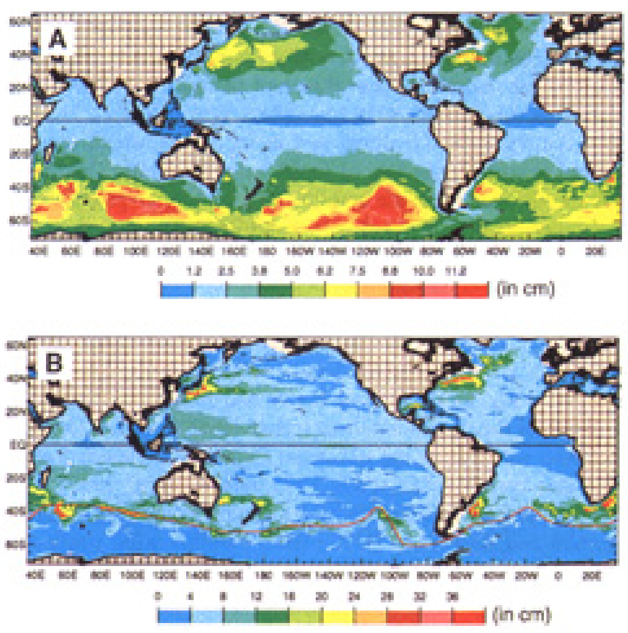

Figure 2. (a.) Non-steric rms SSH variability from simulation BT6. The units are cm and the contour interval is 1.25 cm. (b.) Steric rms SSH variability from simulation BT6. The units are cm and the contour interval is 4 cm. The approximate mean location of the modeled Antarctic Circumpolar Current is depicted in red.

Nonsteric (abyssal layer) variability constitutes a large fraction of the total global RMS SSH variability in simulation BT6, as is shown in Figure 1. Over 37% of the world ocean, the nonsteric component accounts for > 50% of the total variability in this simulation, predominantly at mid and high latitudes. The non-steric variability in this simulation (Figure 2a) results from three potential driving mechanisms [*Hurlburt and Metzger,* 1998]: direct forcing by temporal variations of the wind stress [*Brink*, 1989; *Niller et al.*, 1993; *Fukumori et al.*, 1998; *Stammer et al.*, 2000], vertical mixing and eddy-driven deep flows resulting from baroclinically unstable upper ocean currents [*Rhines and Holland*, 1979; *Hurlburt et al.*, 1996]. The resulting flow is strongly influenced by the *f/h* contours of the bottom topography. The remainder of this section will address these mechanisms, focusing on the eddy-driven deep flow mechanism.

Hurlburt and Metzger [1998] discuss high abyssal eddy kinetic energy (EKE) associated with high upper ocean EKE as one indicator of baroclinic instability, a mesoscale surface flow instability that can efficiently transfer upper ocean energy into the abyssal layer. Observationally, upper ocean variability maxima in the Agulhas, Gulf Stream and Kuroshio regions have been shown to coincide with regions of high abyssal EKE calculated using data from current meter moorings [*Schmitz*, 1984, 1996; *Hurlburt et al.*, 1996; *Hurlburt and Hogan*, 2000]. The approximate collocation of specific upper and abyssal ocean mesoscale anomalies, with the upper anomaly driving the abyssal was noted in observations in the Gulf Stream region by *Savidge and Bane* [1999]. Therefore, by comparing the locations of the non-steric variability maxima (Figure 2a) with the steric (upper ocean) maxima (an indicator of a surface flow instability, Figure 2b), we can largely determine which non-steric maxima are the result of eddy-driven deep flows. This determination is greatly facilitated by the very different patterns of steric SSH variability (Figure 2b) and wind-driven non-steric variability (Figure 3), even in the Antarctic region. Figure 3 is from barotropic simulation BT1.

Non-steric variability maxima (Figure 2a) in the Agulhas retroflection, Antarctic Circumpolar Current, Brazil-Malvinas confluence, East Australian Current, Gulf Stream and Kuroshio regions all coincide with steric variability maxima (Figure 2b). Since these features (1) occur in regions of high mesoscale variability and (2) do not coincide with large wind-driven non-steric variability (Figure 3) nor with local vertical mixing extrema (not shown), we have strong indication that these features are due to eddy-driven deep flows resulting from baroclinic instability. In these regions the eddy-driven deep flow contribution to the non-steric variability typically ranges between 5 – 10 cm rms, but several areas show contributions greater than 10 cm rms.

In the Gulf Stream region, even 1/16° resolution is not enough for accurate simulation of the variability [*Hurlburt and Hogan,* 2000]. However, they included a 1/64° Atlantic simulation and they showed that it does give a realistic pattern and amplitude for Gulf Stream SSH variability in comparison with TOPEX/POSEIDON altimeter data and realistic abyssal EKE in comparison with calculations from current meter data presented by *Schmitz* [1984]. When we calculated the non-steric contribution to SSH from this simulation (not shown), the resulting rms variability was about 25% of the total in the Gulf Stream region with maxima exceeding 10 cm rms. We also found that the range in non-steric SSH exceeds 30 cm in synoptic snapshots. Since this simulation was driven by the HR monthly wind stress climatology (unlike simulations BT1 and BT6, which were forced 1979-97 by ECMWF 1000 mb winds), any wind driven contribution to this non-steric variability is small.

At high latitudes throughout the world ocean there are broad areas of high non-steric variability (Figure 2a) which are not the result of upper ocean eddy-driven deep flows. This high frequency variability is due to a wind-driven non-steric contribution to the barotropic mode (Figure 3). The result depicted in Figure 3 is from a 1-layer barotropic analog of BT6 (simulation BT1). Figure 3 is similar in both distribution and amplitude to the barotropic model results of *Stammer et al.* [2000]. As they discuss, this wind-driven contribution is high frequency in relation to satellite altimeter repeat cycles and is thus an important source of aliasing in altimeter SSH data. Since this contribution is a largely deterministic response to wind forcing, they also demonstrate that it can be at least partially removed from the altimeter data using a wind-driven barotropic model.

Summary and Conclusions

A pair of world ocean simulations are used to investigate the effects of mesoscale flow instabilities on the non-steric contribution to the global barotropic mode. The simulations use horizontal resolution of 1/16° for each variable and vertical resolution of 1 (simulation BT1) and 6 (BT6) layers, both with realistic topography. The two simulations were forced 1979-97 by 6-12 hourly 1000mb winds from the European Centre for Medium-Range Weather Forecasts.

Nonsteric variability constitutes a large fraction of the total global RMS SSH variability in simulation BT6, as is shown in Figure 1. Over 37% of the world ocean the nonsteric component accounts for > 50% of the total variability, predominantly at mid and high latitudes. The non-steric (abyssal layer) contribution to the barotropic mode in the model contains variability resulting from three potential mechanisms [*Hurlburt and Metzger*, 1998]: direct forcing by temporal variations of the wind stress [*Brink*, 1989; *Niller et al.*, 1993; *Fukumori et al.*, 1998; *Stammer et al.*, 2000], vertical mixing and eddy-driven deep flows resulting from baroclinic vortex compression and stretching, especially that resulting from baroclinic instability of upper ocean currents [*Hurlburt et al.*, 1996].

Hurlburt and Metzger [1998] discuss high abyssal EKE associated with high upper ocean EKE as being one indicator of baroclinic instability, a mesoscale surface flow instability that can efficiently transfer upper ocean energy into the abyssal layer. Figures 2 and 3 show global maps of steric and non-steric contributions to SSH variability simulated by model experiments BT1 (Figure 3) and BT6 (Figure 2). By comparing the locations of the non-steric (abyssal) variability maxima (Figure 2a) with the steric (upper ocean) maxima (an indicator of a surface flow instability, Figure 2b) and with the wind-driven non-steric contribution to SSH variability (Figure 3), we can largely determine which non-steric maxima are the result of eddy-driven deep flows.

Non-steric variability maxima (Figure 2a) in the Agulhas retroflection, Antarctic Circumpolar Current, Brazil-Malvinas confluence, East Australian Current, Gulf Stream and Kuroshio regions all coincide with steric variability maxima (Figure 2b). Since these features (1) occur in regions of high mesoscale variability and (2) do not coincide with large wind-driven non-steric variability nor with local vertical mixing extrema (not shown), we have strong indication that these features are due to eddy-driven deep flows resulting from baroclinic instability (actually a mixed baroclinic - barotropic instability). In these regions the eddy-driven deep flow contribution to the non-steric variability ranges between 5 – 10 cm rms, and in a few areas is higher than 10 cm rms. In addition, a 1/64° Atlantic model with realistic Gulf Stream region SSH variability and abyssal EKE showed related non-steric SSH variability that is about 25% of the total and a range in non-steric SSH exceeding 30 cm in synoptic snapshots.

In eddy-resolving nowcasting and forecasting it is essential to know the eddy-driven non-steric (abyssal) contribution to the barotropic mode and its corresponding contribution to SSH. Since altimeter data includes both steric and non-steric contributions to SSH, it is necessary to distinguish these SSH components in the mapping of steric upper ocean features and the associated downward projection of the SSH data. In forecasting of mesoscale oceanic features, it is essential to initialize these features at all depths, including the abyssal ocean [*Hurlburt et al.*, 1990]. In the assimilation of altimeter data, the preceding requirements can only be met by using a fully eddy-resolving ocean model which demonstrates the essential mesoscale dynamics. Further, a data-assimilative model is needed due to the nondeterministic nature of the flow instabilities driving the associated non-steric variability.

Acknowledgements. This work was sponsored by the Office of Naval Research (program element 601153N) as part of the project "Thermodynamic and Topographic Forcing in Global Ocean Models". The computations in this paper were completed utilizing grants of computer time from the Defense Department High Performance Computing (HPC) Modernization Office on the CEWES and NAVO Cray T3Es. This includes time under DoD Challenge grants for the 1/16° 6-layer global and 1/64° Atlantic simulations. The model development work and computational assistance of Alan Wallcraft are noted and appreciated. This is contribution NRL/JA/7323—99-0050 .

References

Brink, K. H., Evidence for wind-driven current fluctuations in the western North Atlantic, *J. Geophys. Res.*, *94*, 2029-2044, 1989.

European Centre for Medium-Range Weather Forecasts (ECMWF), User guide to ECMWF products, *Meteorol. Bull. M3.2*, Reading, England, 1995.

Fukumori, I., R. Ragunath, and L.L. Fu, Nature of global large-scale sea level variability in relation to atmospheric forcing: a modeling study, *J. Geophys. Res.*, *103*, 5493-5512, 1998.

Gibson, J. K., P. Kållberg, S. Uppala, A. Hernandez, A. Nomura, and E. Serrano, ECMWF re-analysis project report series: 1. ERA description, ECMWF, Reading, Berkshire, UK, 72 pp., 1997.

Hellerman, S. and M. Rosenstein, Normal monthly wind stress over the world ocean with error estimates, *J. Phys. Oceanogr.*, *13*, 1093-1104, 1983.

Hogan, P.J. and H.E. Hurlburt, Impact of upper ocean – topographic coupling and isopycnal outcropping in Japan/East Sea models with 1/8° to 1/64° resolution, *J. Phys. Oceanogr.*, 2000, (in press).

Holland, W. R., and L. B. Lin, On the generation of mesoscale eddies and their contribution to ocean general circulation, I, A preliminary numerical experiment, *J. Phys. Oceanogr*, *5*, 642-657, 1975.

Hurlburt, H. E., and J. D. Thompson, A numerical study of Loop Current intrusions and eddy-shedding, *J. Phys. Oceanogr.*, ***10***, 1611-1651, 1980.

Hurlburt, H.E., D.N. Fox, and E.J. Metzger, Statistical inference of weakly correlated subthermocline fields from satellite altimeter data, *J. Geophys. Res.*, *95*, 11375-11409, 1990.

Hurlburt, H. E., A. J. Wallcraft, W. J. Schmitz Jr., P. J. Hogan, and E. J. Metzger, Dynamics of the Kuroshio/Oyashio current system using eddy resolving models of the North Pacific Ocean, *J. Geophys. Res.*, *101*, 941-976, 1996.

Hurlburt, H. E. and E. J. Metzger, Bifurcation of the Kuroshio Extension at the Shatsky Rise, *J. Geophys. Res.*, *103*, 7549-7566, 1998.

Hurlburt, H. E., and P. J. Hogan, Impact of 1/8° to 1/64° resolution on Gulf Stream model-data comparisons in basin-scale subtropical Atlantic Ocean models, *Dyn. Atmos. Oceans.*, 2000, (in press).

Mesinger, F., and A. Arakawa, *Numerical Methods Used in Atmospheric Models*. GARP Publ. Ser., no. 17, WMO, 64 pp., 1976.

Metzger, E. J., H. E. Hurlburt, J. C. Kindle, Z. Sirkes, and J. M. Pringle, Hindcasting of wind driven anomalies using a reduced-gravity global ocean model, *Mar. Technol. Soc. J.*, *26(2)*, 23-32, 1992.

Moore, D.R. and A.J. Wallcraft, Formulation of the NRL layered ocean model in spherical coordinates, *NRL CR 7323--96-0005*, Nav. Res. Lab., Stennis Space Center, MS, 24 pp., 1998.

National Oceanic and Atmospheric Administration, ETOP05 digital relief of the surface of the earth, *Data Announce. 86-MGG-07*, Nat. Geophys. Data Cent., Washington, D.C., 1 p., 1986.

Niller, P. P., J. Filloux, W. T. Liu, R. M. Samelson, J. P. Paduan, and C. A. Paulson, Wind-forced variability of the deep eastern North Pacific: observations of seafloor pressure and abyssal currents, *J. Geophys. Res.*, *98*, 22589-22602, 1993.

Rhines, P. B., and W. R. Holland, Theoretical discussion of eddy-driven mean flows, *Dyn. Atmos. Oceans*, *3*, 289-325, 1979.

Savidge, D. K., and J. M. Bane Jr., Cyclogenesis in the deep ocean beneath the Gulf Stream 2. dynamics, *J. Geophys. Res.*, *104*, 18127-18140, 1999.

Schmitz, W. J. Jr., Abyssal eddy kinetic energy in the North Atlantic, *J. Mar. Res.*, *42*, 509-536, 1984.

Schmitz, W. J. Jr., On the eddy field in the Agulhas Retroflection, with some global considerations, *J. Geophys. Res.*, *101*, 16259-16271, 1996.

Stammer, D., C. Wunsch and R. M. Ponte, De-aliasing of global high frequency barotropic motions in altimeter observations, *Geophys. Res. Letters*, *27*, 1175-1178, 2000.

Suginohara, N., Quasi-geostrophic waves in a stratified ocean with bottom topography, *J. Phys. Oceanogr.*, *11*, 107-115, 1981.

Wallcraft, A. J., The Navy Layered Ocean Model users guide, *NOARL Rep. 35*, 21 pp., Nav. Res. Lab., Stennis Space Center, Miss., 1991.

Wallcraft, A.J. and D.R. Moore, The NRL Layered Ocean Model. *Parallel Computing*, *23*, 2227-2242, 1997.

J. F. Shriver and H. E. Hurlburt, Naval Research Laboratory, Code 7323, Stennis Space Center, Mississippi, 39529. (e-mail: shriver@nrlssc.navy.mil)

(Received October 12, 1999; revised April 18, 2000; accepted July 13, 2000)